Earth's Future

RESEARCH ARTICLE
10.1029/2021EF002414

Future Flood Risk Exacerbated by the Dynamic Impacts of Sea Level Rise Along the Northern Gulf of Mexico

M. V. Bilskie[1], D. Del Angel[2], D. Yoskowitz[2], and S. C. Hagen[3,4]†

[1]School of Environmental, Civil, Agricultural, and Mechanical Engineering, University of Georgia, Athens, GA, USA, [2]Texas A&M University-Corpus Christi, Harte Research Institute, Corpus Christi, TX, USA, [3]Department of Civil and Environmental Engineering, Louisiana State University, Baton Rouge, LA, USA, [4]Center for Computation and Technology, Louisiana State University, Baton Rouge, LA, USA

Abstract A growing concern of coastal communities is increased flood risk and non-monetary consequences due to climate-induced impacts such as sea level rise (SLR). Previous efforts have discussed the importance of future flood risk quantification using broad aggregations of monetary loss with "bathtub" SLR models rather than more physically based modeling approaches. Here we quantify actual impacts to coastal communities at the census block level using a dynamic, high-resolution, bio geophysical modeling framework for four SLR scenarios for the year 2100. This framework accounts for future sea-levels, landscape change, and urbanization to quantify the 1% and 0.2% annual exceedance probability (AEP) water levels. The computed AEP water levels were used to quantify building damage and populations of displaced people and people requiring long-term shelter across the Northern Gulf of Mexico (NGOM) (Mississippi, Alabama, and the Florida panhandle). The increase in damaged buildings under SLR is linear, with an increase of 16,367 damaged buildings per 1 m of SLR ($R^2 = 0.96$) for the 1% AEP flood. The rate increases to 24,981 damaged buildings per 1 m of SLR ($R^2 = 0.96$) for the 0.2% AEP, on average. The increase in displaced people across the NGOM is 8,056 people per meter of SLR, and people requiring shelter is 300 per meter of SLR. The results in this work highlight the varying levels of risk across the NGOM and the change in risk under climate change-induced impacts.

Key Points:

- Building damage rates are 16,367 and 24,981 per meter of sea level rise (SLR) for the 1% and 0.2% annual exceedance probability flood
- Displaced people and people requiring shelter increase by 8,056 and 300 per meter of SLR, respectively
- The number of displaced people per decade increases by 1,208 (or 121 per year from 2020 to 2100) under a SLR increase of 1.2 m

Correspondence to:
M. V. Bilskie,
mbilskie@uga.edu

Citation:
Bilskie, M. V., Angel, D. D., Yoskowitz, D., & Hagen, S. C. (2022). Future flood risk exacerbated by the dynamic impacts of sea level rise along the Northern Gulf of Mexico. *Earth's Future*, *10*, e2021EF002414. https://doi.org/10.1029/2021EF002414

Received 13 SEP 2021
Accepted 28 MAR 2022

Author Contributions:
Conceptualization: M. V. Bilskie, D. Yoskowitz, S. C. Hagen
Funding acquisition: S. C. Hagen
Methodology: M. V. Bilskie, D. Del Angel
Project Administration: S. C. Hagen
Supervision: D. Yoskowitz, S. C. Hagen
Visualization: M. V. Bilskie
Writing – original draft: M. V. Bilskie
Writing – review & editing: M. V. Bilskie, D. Del Angel, D. Yoskowitz, S. C. Hagen

1. Introduction

The 1% and 0.2% annual chance flood (commonly referred to as the 100- and 500 year flood, respectively) have been used as guides in the United States for planning and development decisions and to inform the public on flood insurance premiums. These flood protection metrics have proven inefficient in resilience planning, especially in an uncertain future (Highfield et al., 2013; Linkov et al., 2014). As a result, flood policy has shifted from flood protection to floodplain management. This paradigm attempts to mitigate flood hazards and reduce at-risk elements and their susceptibility rather than solely focus on the hazard (Messner & Meyer, 2006; Meyer et al., 2009). Flood risk is defined as a measure that combines a flood hazard(s) with exposure and is the probability that damage may occur over a certain period (i.e., expected annual damage (EAD)). Flood hazard is the likelihood a flood event may occur (e.g., 1% annual chance flood), and flood exposure is the at-risk elements to flooding (Kron, 2005; Merz et al., 2010; Meyer et al., 2009).

Predicting the future spatial distribution and depth of flood hazards and risk quantification is a challenge given climate non-stationarity and uncertainty (Oddo et al., 2020; Rohmer et al., 2021). However, it is essential to include trajectory changes instead of steady-state or historical baselines for floodplain and coastal resources management (Chapin et al., 2009). Historically, growing coastal populations have been the main driver of increased flood risk (Bouwer, 2011; Muis et al., 2016). However, rising sea levels will play a more substantial role in amplifying flood risk (Habete & Ferreira, 2017; Hallegatte et al., 2013). Consequently, there is a need to quantify flood hazards, exposure, and risk using projections of future sea levels and landscapes.

Flood hazard and risk has been quantified across local, regional, national (Genovese et al., 2011; Hallegatte, 2007; Heberger et al., 2011) and global scales (Hallegatte et al., 2013; Jongman et al., 2012; Muis et al., 2016; Neumann et al., 2015; Shepard et al., 2012). However, studies spanning large regions rely on broad aggregations of depth-damage relationships and coarse hydrodynamic models (and potentially limited physics) or tide gauge records at broadly spaced locations. In contrast, regional and local studies benefit from detailed socio-economic information and may engage more complex hydrodynamic models. Previous work has focused on a single (often

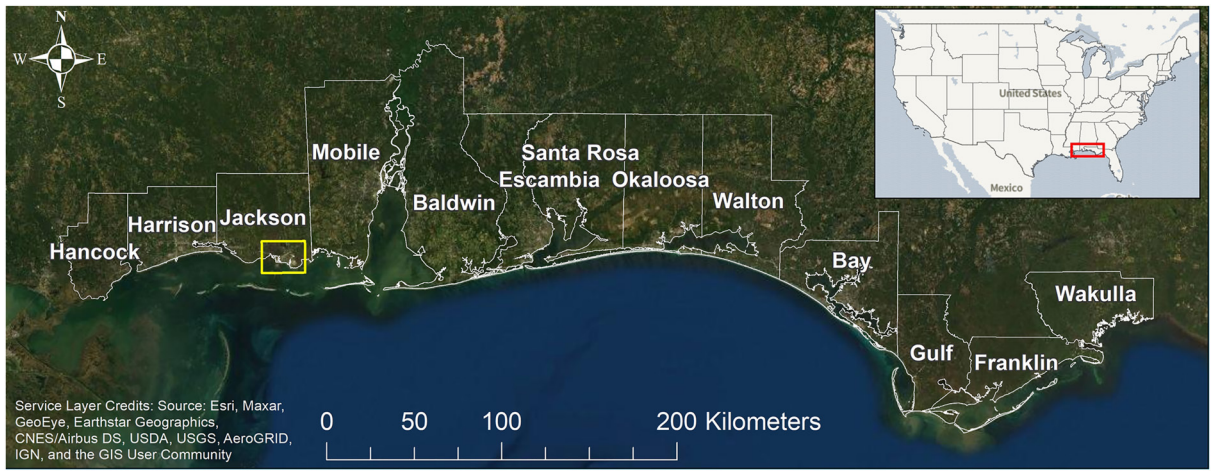

Figure 1. Map of the study area along the Northern Gulf of Mexico coast. The yellow box is the inset shown in Figure 2.

historical) storm or range of storms that follow the Saffir-Simpson scale. This approach does not reflect the wide range of potential flooding scenarios (Hagen & Bacopoulos, 2012) and does not include the effects of climate change beyond sea level rise (SLR) (Irish et al., 2010; Passeri, Hagen, Medeiros, Bilskie, Alizad, et al., 2015). Furthermore, it is computationally expensive to employ contemporary, high-resolution, coastal inundation models to derive probabilistic flood depth surfaces (e.g., 1% annual chance flood) for large (multi-state) regions.

Coastal flood hazard modeling has experienced considerable advancements in the last several years, specifically in including the role of climate change and SLR on elevated peak storm surges using high-resolution hydrodynamic models (Bilskie, Hagen, Alizad et al., 2016; Bilskie et al., 2019; Smith et al., 2010; Tebaldi et al., 2012; Woodruff et al., 2013). Flood hazard studies did not account for the effects of SLR on flood depths and considered SLR only as a linear superposition to current flood hazard information. Methods involving a linear increase in flood depths for a given SLR, commonly referred to as a bathtub model, neglect the non-linear and spatio-temporal changes in flood levels, specifically across the coastal landscape in normally dry regions (within populated areas). Such changes in flood levels are substantial and do not always increase by a given SLR amount (Bilskie & Hagen, 2018; Bilskie, Hagen, Alizad et al., 2016; Bilskie et al., 2019; Hagen et al., 2017; Liu et al., 2019; Passeri, Hagen, Medeiros, Bilskie, Alizad, et al., 2015; Plant et al., 2016). Therefore, the Coastal Dynamics of Sea Level Rise (CDSLR) framework was established. CDSLR enhances coastal flood hazard quantification under climate change conditions, focusing on SLR and long-term biogeophysical changes (Hagen et al., 2017; Kidwell et al., 2016). The CDSLR framework, including geomorphic change assessment, are discussed in detail in Plant et al. (2016), Alizad, Hagen, Morris, Bacopoulos et al. (2016), Alizad et al. (2018), Bilskie et al. (2019), Bilskie et al. (2014), Bilskie, Hagen, Medeiros et al. (2016), DeLorme et al. (2016), Hagen et al. (2017), Kidwell et al. (2016), Medeiros et al. (2015), Passeri, Hagen, Bilskie, and Medeiros (2015), Passeri et al. (2014); Passeri, Hagen, Medeiros, and Bilskie (2015), Passeri, Hagen, Medeiros, Bilskie, Alizad, et al. (2015), and Passeri et al. (2016).

This study aims to extend the CDSLR approach to quantify flood risk across 13 coastal counties in Mississippi, Alabama, and the Florida panhandle (Figure 1). This multi-state region includes 4,900 km (3,000 miles) of open coast shoreline, a dozen bays, major rivers, and extensive coastal infrastructure, including a large tourism industry. Here, we focus on residential building counts, displaced people, and people requiring shelter at the census block level.

The following sections are outlined as follows. Section 2 describes the CDSLR biogeophysical modeling and flood risk quantification approach. Flood risk results are presented in Section 3, a discussion follows in Section 4, and a summary and conclusions are in Section 5.

2. Methods and Data

2.1. Flood Hazard Model

The simulations of coastal flooding utilized an ADvanced CIRCulation + Simulating Waves Nearshore (ADCIRC + SWAN) model of the Northern Gulf of Mexico (NGOM; Bilskie, Hagen, Medeiros et al., 2016). ADCIRC is governed by a depth-integrated form of the shallow water equations to solve for water levels and currents on an unstructured finite element mesh (Dawson et al., 2006; Kinnmark, 1985; Kolar et al., 1994; Luettich & Westerink, 2004; Westerink et al., 2008). SWAN is governed by the wave action balance equation and represents the wavefield as a phase-average spectrum (Booij et al., 1999). ADCIRC and SWAN are tightly coupled and utilize the same unstructured mesh (Dietrich et al., 2011; Zijlema, 2010). ADCIRC was run using a 1 s time-step and SWAN with a 600 s time-step (also the ADCIRC + SWAN coupling interval). The unstructured finite element mesh of the NGOM contains 5.5 million nodes and includes horizontal spatial resolution as fine as 15 m in narrow channels. Generally, the model resolution is between 40 and 150 m across the coastal floodplain up to the 15 m elevation contour. The most recent topographic and bathymetric datasets were used in the construction of the unstructured mesh at the time the mesh was developed (2012–2015). In Mississippi, topographic data was obtained from pre-Katrina Lidar surveys, and data for Alabama and Florida was from 2006 to 2009 Lidar.

The mesh was design with careful consideration for mesh node placement and alignment of element edges along sharp gradients in elevation such as roadways, railroads, natural ridges (i.e., vertical features), and dredged channels (Bilskie & Hagen, 2013; Bilskie et al., 2015). This model setup was validated for Hurricanes Ivan (2004), Dennis (2005), Katrina (2005), and Isaac (2012) with a combined regression line slope of 0.98 and R^2 of 0.96 when comparing simulated to measured peak water levels (Bilskie, Hagen, Alizad et al., 2016; Bilskie, Hagen, Medeiros et al., 2016).

The ADCIRC + SWAN model was forced by 219 synthetic tropical cyclones that represent a range of storm climatology across the NGOM. The storm parameters (track and intensity) were derived by the Joint Probability Method with Optimum Sampling approach (Resio, 2007; Resio et al., 2009; Toro et al., 2010). The synthetic storms are described by central pressure deficit, radius to maximum winds, forward velocity, storm heading, and landfall location (Niedoroda et al., 2010). The storms are characterized by these values with the likelihood of a particular storm occurring given a combination of the parameters. The combination of parameters is obtained by historical observations from the period around 1940–2006. Future storm climatology and rainfall-runoff was not included in this study. The storm selection process is outlined in Bilskie et al. (2019).

Water levels were simulated for each of the 219 storms for five sea level conditions—present day and four global SLR scenarios for the year 2100. The SLR scenarios, prescribed by Parris et al. (2012), were low (0.2 m), intermediate-low (0.5 m), intermediate-high (1.2 m), and high (2.0 m) with a baseline year of 1992. The ADCIRC + SWAN model reflects a particular landscape based on an individual SLR scenario. The coastal landscape was modified for each SLR scenario (and associated sea level rate of change and carbon emission) and includes salt marsh, beach width (erosion or accretion), dune height, and land use land cover (LULC; Alizad, Hagen, Morris, Medeiros et al., 2016; Passeri et al., 2016; Plant et al., 2016). Therefore, an individual model mesh for each sea level is considered, which totals five landscape configurations (present-day, low, intermediate-low, intermediate-high, and high). Details regarding the landscape modification can be found in Bilskie, Hagen, Alizad et al. (2016). Adjusting the landscape for various SLR scenarios is a key component of the CDSLR approach.

A total of 1,095 storm surge simulations took place (219 storms × 5 mean sea level conditions). The maximum simulated water elevation across the model domain (i.e., each computational mesh node) was saved for each storm event. The maximum water levels were ranked, sorted, and then multiplied by each synthetic storm's probability of occurrence. This calculation leads to water level as a function of annual exceedance probabilities. From this data set, the 1% and 0.2% annual chance stillwater storm surge heights were obtained for each SLR scenario (Bilskie et al., 2019). The 1% and 0.2% annual chance stillwater maps are available at gomsurge.org.

2.2. Exposure and Vulnerability Modeling

This work utilized HAZUS-MH V 3.2 to assess the socio-economic impacts of storm surge under SLR. HAZUS-MH is a Geographic Information System based modeling tool developed by the Federal Emergency

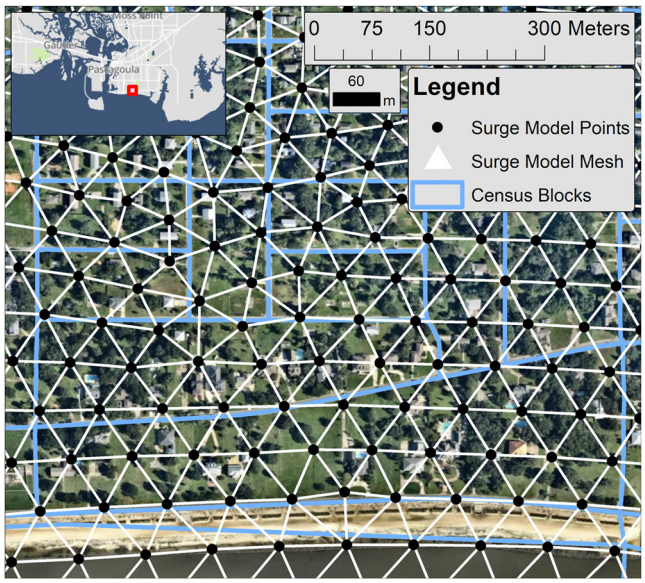

Figure 2. An example representation of the storm surge model discretization (i.e., resolution) with the census blocks for a region in the Pascagoula, MS in Jackson County, MS (see yellow inset in Figure 1). The census blocks (blue) can span a few hundred meters and contain numerous storm surge model points (black) and mesh elements (white). The storm surge model's horizontal spatial resolution is ~60 m in this region of Pascagoula, MS.

Management Agency to estimate physical, economic, and social impacts of natural disasters such as floods, earthquakes, and hurricanes. HAZUS includes a database with aggregated and site-specific inventory that contains demographics, general building stock, agricultural statistics, vehicle inventory, essential facilities, transportation systems, and utility systems (among other sensitive facilities). These data can be manipulated and enhanced by user-specified information (Federal Emergency Management Agency (FEMA), 2013). The ability to perform multiple layers of analysis and incorporate user-developed data into HAZUS makes this an easy-to-use, low-cost, and flexible tool for adaptation planning (Banks et al., 2014).

The annual exceedance probability (AEP) stillwater flood extent and depths from the coastal flood model (described in Section 2.1) were used to identify exposed building assets and estimate the damage. The HAZUS building stock inventory is based on data from the U.S. Census and commercial enterprises data by Dun and Bradstreet. The HAZUS Flood Module applies depth-damage curves from the Federal Insurance Administration and the U.S. Army Corps of Engineers to assess damage (Scawthorn et al., 2006). These damage curves consider building type, first-floor elevation, and design level (pre or post- Flood Insurance Rate Maps) to estimate percent damage as a function of flood depth. Buildings are classified as substantially damaged if building damage is greater than or equal to 50% of the building cost (herein, we refer to substantially damaged buildings as damaged buildings). Building damage cost is derived from building construction estimates published in Mean Square Foot Costs (R.S. Means) using 2014 Values (Federal Emergency Management Agency (FEMA), 2013; Zuzak et al., 2018). Losses are calculated by census blocks (Figure 2) and presented as area-weighted estimates of damage, where cost is considered a percent of the replacement cost (Scawthorn et al., 2006). Output reported in this publication includes total replacement cost for buildings for both pre-and post-FIRM structures.

In addition to building damage, socio-economic impacts were quantified at each census block. The inundation area determined the number of displaced individuals and households. People are considered displaced regardless of building damage. A threshold flood depth of 6 inches (which corresponds to a typical curb height) was used to determine the inability to travel into an area (Federal Emergency Management Agency (FEMA), 2013). A population database is part of the HAZUS inventory and is based on the 2010 U.S. Census. The HAZUS model also estimates displaced people that will require temporarily lodging in shelters. The shelter algorithm uses a shelter category weight for income (weight = 0.8) and age (weight = 0.2) with a relative modification factor for income to determine population statistics (for more information, see Equation 13–15 and 13–16 in Federal Emergency Management Agency (FEMA), 2013).

Increases in population and development were not incorporated in future scenarios. Instead, the results portray the current and potential change in socio-economic impact to existing communities.

2.3. Risk Quantification

Flood risk is defined as a measure that combines flood hazard with exposure, which is the probability that damage may occur over a given year and results in EAD (Meyer et al., 2009). EAD is typically quantified in monetary losses. However, it is also important to consider the spatial distribution of social risk. Therefore, we focus on the actual impacts of flooding on property damages (i.e., substantially damaged buildings), displaced people, and people requiring shelter during a tropical cyclone event. For flood risk assessments, flood damages must be quantified for a set of flood events representing a given AEP (or return period) to create a flood damage-probability curve (Figure 3a). The flood risk represented by the EAD is the area under the flood damage-probability curve (Meyer et al., 2009). The trapezoidal rule was used to compute EAD given a set of damages for specific AEP events. EAD was quantified from damage exposure to the 0.2%, 1%, and 100% chance AEP (coastal inundation modeling and HAZUS modeling described in Sections 2.1 and 2.2, respectively) using the trapezoidal rule to estimate the area under the flood damage-probability curve. We assume that no damage occurs with the 100%

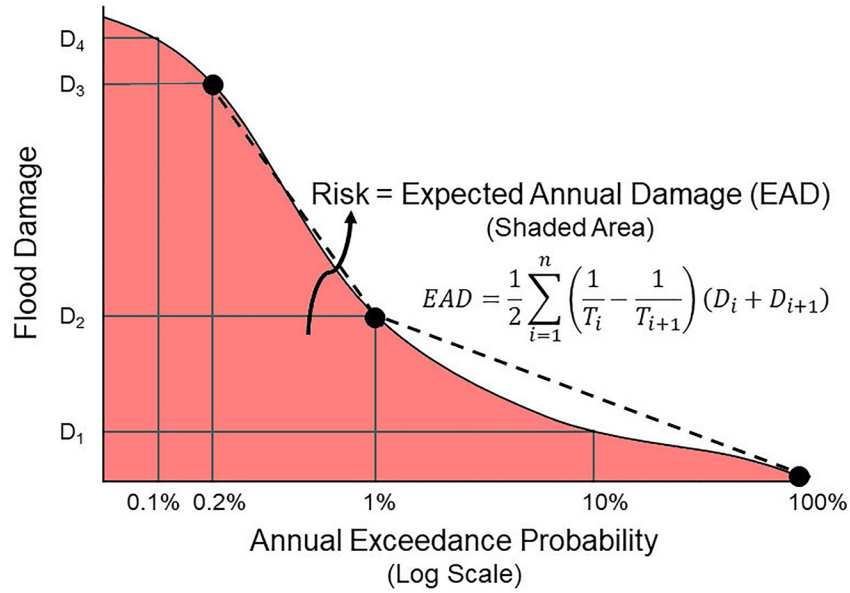

Figure 3. Example of risk calculation as defined as the estimated expected annual damages (EAD). EAD is computed using the trapezoidal rule where T is return period, or one divided by the annual exceedance probability (AEP) ($T = 1/AEP$), D is damage for a specific AEP, and n is the number of AEP so all relevant events are included (Olsen et al., 2015). The x-axis is in log-scale (base 10). The figure was inspired and adapted based on Figure 1 of Meyer et al. (2009).

AEP. The calculation of the EAD occurs for (a) substantially damaged buildings, (b) displaced people, and (c) people requiring shelter. The results of the risk assessment yield the expected annual average number of buildings substantially damaged, annual number of affected people that will be displaced, and the expected annual number of affected people that will require shelter.

3. Results

3.1. Annual Exceedance Probability (AEP) Stillwater Elevations

The coastal flood hazard across the NGOM is illustrated by the 1% (i.e., 1 in 100 year) and 0.2% (i.e., 1 in 500 year) AEP stillwater elevations for present day and four SLR scenarios (Figures 4 and 5). Stillwater surge heights across the Alabama and Florida Panhandle are relatively modest but increase under SLR, particularly near Mobile, AL, Pensacola, and Panama City, FL. Stillwater surges heights for the 0.2% AEP are greater than 6 m NAVD88 near Mobile, AL and 5–6 m NAVD88 near Destin and Panama City, FL are for the high SLR scenario (2.0 m).

The highest stillwater elevations occur along the Mississippi coast (Hancock, Harrison, and Jackson Counties) and near Florida's Big Bend region (Franklin and Wakulla Counties). The 0.2% AEP stillwater surge heights range from 6 to 7 m NAVD88 near Gulfport, MS, and 5–6 m NAVD88 near St. Marks, FL for the low SLR scenario (0.2 m). Coastal Mississippi experiences some of the highest storm surges in the world (e.g., Hurricane Katrina in 2005) due to the wide and flat Mississippi-Alabama outer continental shelf. In Florida's Big Bend, coastally trapped Kelvin waves enhance coastal water levels when storms track parallel to the broad and float west Florida shelf along with funneling effects of surge toward St. Marks (Bilskie, Hagen, Medeiros et al., 2016; Kennedy et al., 2011). Next, we combine the flood hazard results with building stock and socio-economic data to quantify flood consequence and exposure.

3.2. Building Damage Counts

The number of substantially damaged residential buildings for each SLR scenario are shown in Figures 6a and 6b for the full NGOM domain. Over 5,400 and 14,100 residential buildings are damaged under present-day sea level for the 1% AEP and 0.2% AEP flood, respectively. The number of damaged buildings increases with increasing

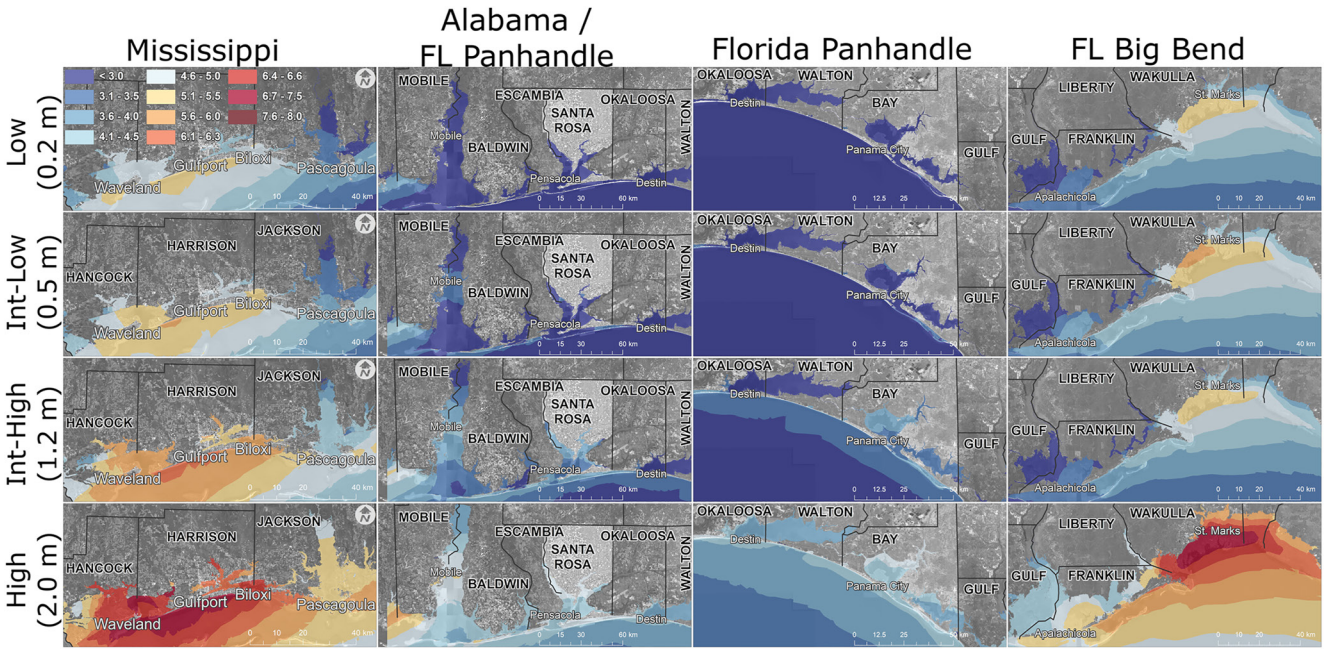

Figure 4. Maps showing the computed 0.1% (B) annual exceedance probability stillwater elevation (m, NAVD88) across the Northern Gulf of Mexico for each sea level rise (SLR) scenario. The SLR scenarios are low (0.2 m) (top row), intermediate-low (0.5 m) (second row), intermediate-high (1.2 m) (third row), and high (2.0 m) (bottom row) (Parris et al., 2012) and reflect the non-linear growth of surge events at the coast.

sea levels and reaches maximum values (2 m of SLR) of over 38,100 (600% increase) and 63,400 (350% increase) for the 1% and 0.2% AEP scenarios. Even at a modest increase in SLR for the intermediate-low scenario (0.5 m SLR) the number of damaged buildings increases by 73% and 62% for the 1% and 0.2% AEP coastal flood events. The increase in damaged buildings is linear, with a slope (rate) of 16,367 damaged buildings per 1 m of

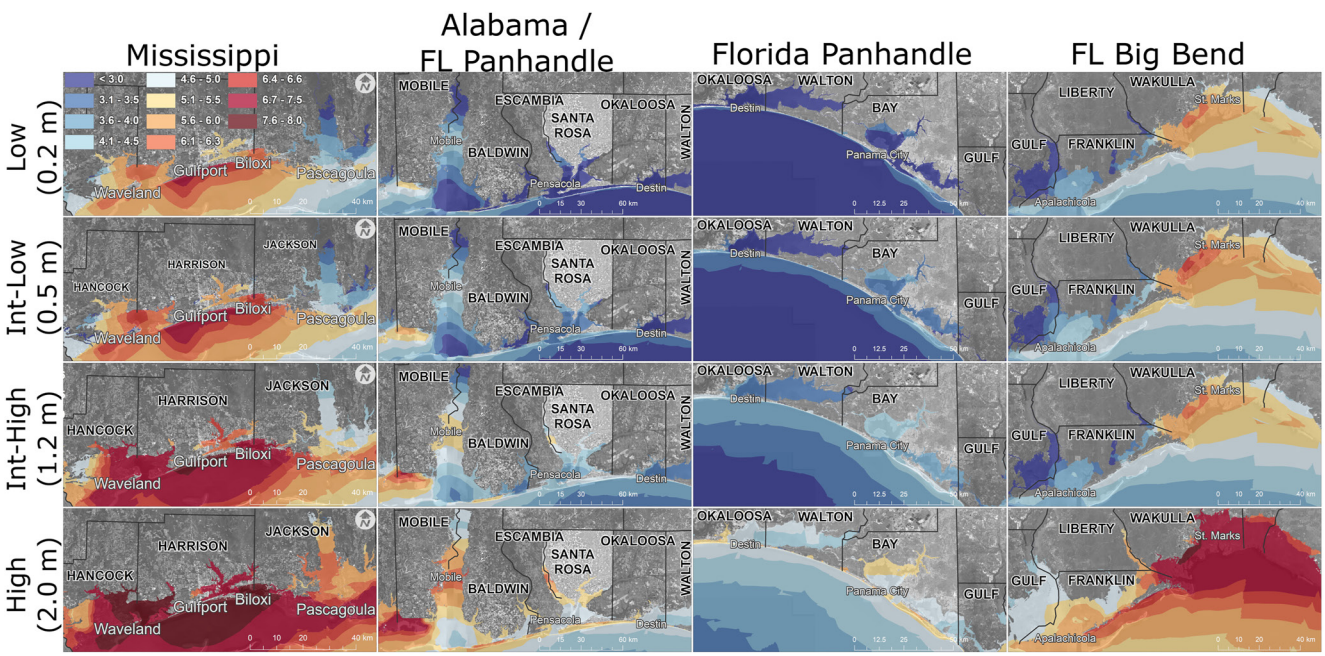

Figure 5. Maps showing the computed 0.2% (B) annual exceedance probability stillwater elevation (m, NAVD88) across the Northern Gulf of Mexico for each sea level rise (SLR) scenario. The SLR scenarios are low (0.2 m) (top row), intermediate-low (0.5 m) (second row), intermediate-high (1.2 m) (third row), and high (2.0 m) (bottom row) (Parris et al., 2012) and reflect the non-linear growth of surge events at the coast.

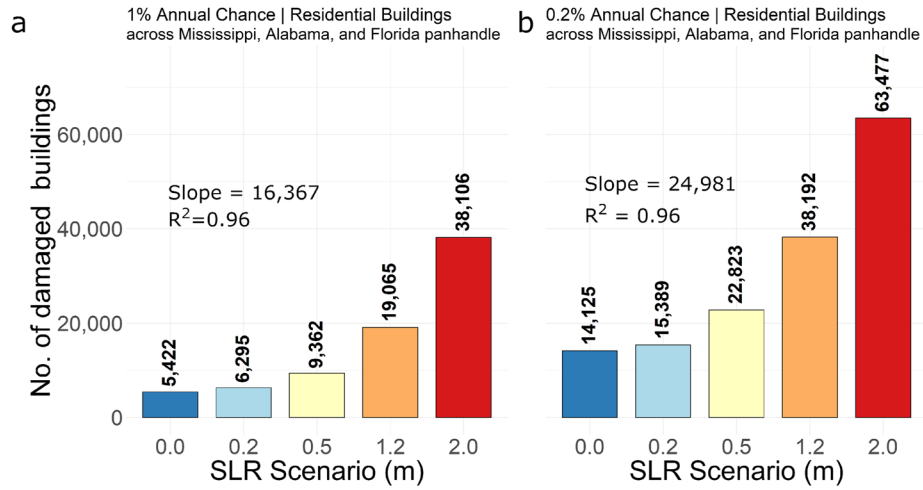

Figure 6. The number of substantially damaged buildings from the (a) 1% and (b) 0.2% annual chance (right) flood extent and depth across the Northern Gulf of Mexico. Substantially damaged buildings are classified as greater than 50% damaged.

SLR (R^2 = 0.96) for the 1% AEP. On average, the rate increases to 24,981 damaged buildings per 1 m of SLR (R^2 = 0.96) for the 0.2% AEP across the entire region.

Next, the number of substantially damaged residential buildings was aggregated across all coastal counties for each SLR scenario from the 1% and 0.2% annual chance flood (Figure 7). These results illustrate where coastal floods are expected to impact residential infrastructure for present and future sea levels. The most significant values of damaged buildings occur along the Mississippi and Alabama coast and in Bay County, FL. Under present-day sea level, Hancock County, MS shows the largest number of damaged buildings at 1,314 for the 1% AEP; however, under the high SLR scenario, the largest damaged building count of 7,400 is found in Jackson County, MS. These counties have some of the highest population densities in the NGOM and feature a high level of exposure to the present 1% annual chance, in contrast to densely populated regions of Mobile County, where presently, there are relatively low counts of damaged buildings for 1% AEP flood (92 buildings).

Similarly, Okaloosa and Escambia Counties, FL have the lowest present-day value of one damaged building, although they feature centers of high-intensity development (e.g., Fort Walton Beach and Pensacola); Gulf County, FL is the lowest under the high scenario at 705 buildings, primarily as a result of low population density in comparison to Bay, Okaloosa, and Escambia counties. Bay County, home to Panama City, features one of the most significant increases in building damage under the intermediate-high and high scenarios. For the 0.2% AEP flood event, the largest damaged building count was found in Harrison County, MS (3,143) for present-day, but Jackson County, MS exceeds all other counties under the high scenario with 13,843 damaged buildings. These results signify that regional hot-spots in flood exposure are substantially altered under varying SLR scenarios and forewarn that regions of low exposure today may not be so in the coming years if population growth continues or increases in the coming decades.

3.3. Flood Risk

Figure 8a displays the flood risk for substantially damaged residential buildings. The units of flood risk in Figure 8a are the expected annual average number of substantially damaged buildings and were summarized at the county level for each SLR scenario. The average increase in building damage per meter of SLR across all counties is 1,128. At present day, Hancock County, MS, has the largest flood risk of 664 buildings. Under the high SLR scenario (2.0 m), Jackson County, MS, yields the highest flood risk of over 3,700 buildings. For all counties, the rate of increasing damaged buildings per meter of SLR is linear as the R^2 (coefficient of determination) of all linear regression lines is greater than 0.90. The rate of change is as high as 1,657 buildings per meter of SLR in Jackson County, MS, and as low as 152 buildings per meter of SLR in rural Wakulla County, FL.

Social flood risk for each county is shown in Figures 8b and 8c in the form of the expected annual average of displaced people (i.e., people may not have access to their homes as a result of flooding [flood depth of 6 inches

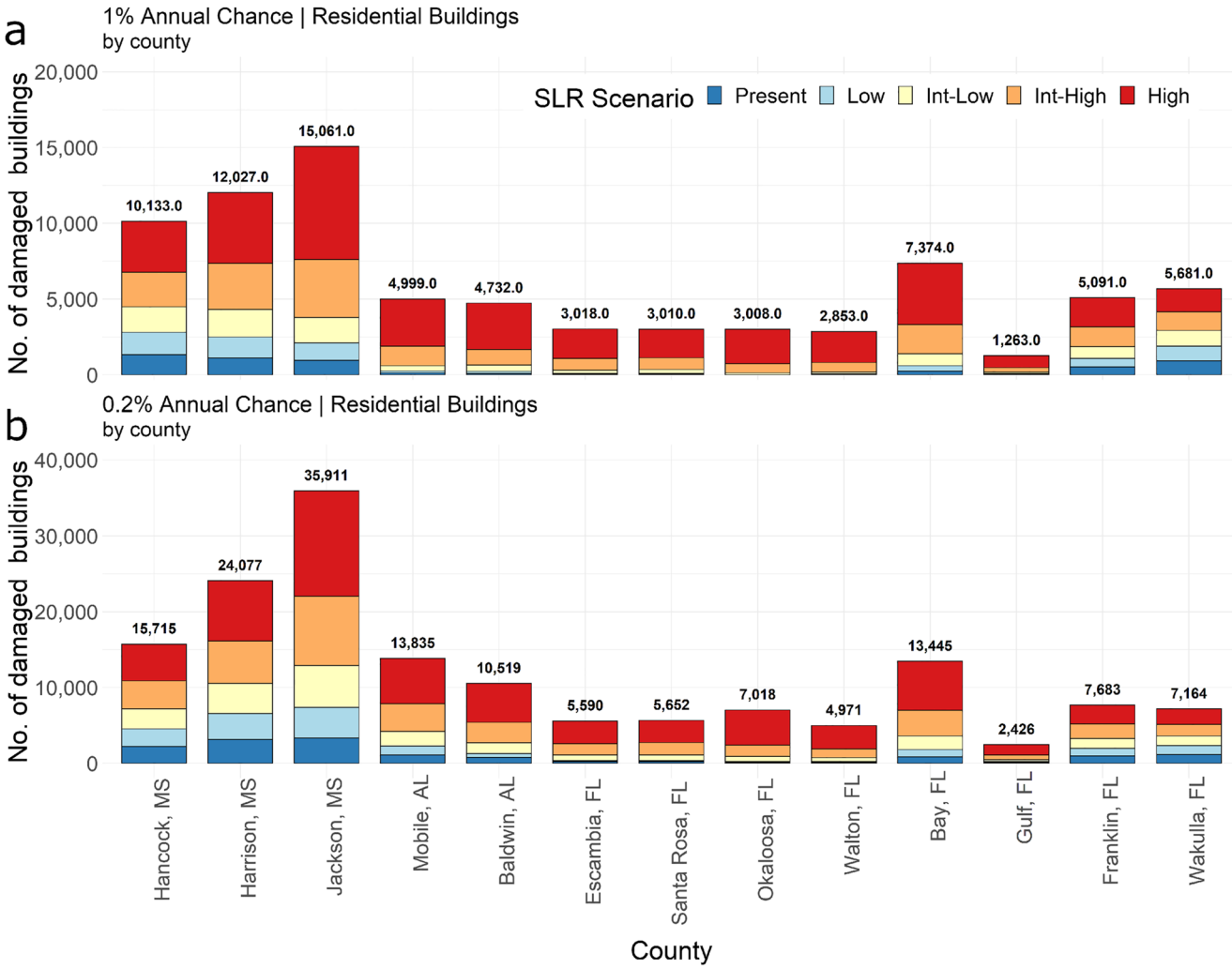

Figure 7. The number of substantially damaged buildings across each coastal county for the (a) 1% and (b) 0.2% annual chance flood. Substantially damaged buildings are classified as greater than 50% damaged. Damages were summed by county. Note the difference in the *y*-axis scale between each panel. The value on top of each bar is the number of damaged buildings under the high (2.0 m) sea level rise scenario.

or more], Federal Emergency Management Agency (FEMA), 2013) and the expected annual average of people requiring temporary accommodations during and post-storm. Western NGOM counties have a larger risk of displaced people than eastern counties (except for Bay County, FL), and follow the pattern of the largest levels of inundation in the AEP floods. Along the east edge of the NGOM, in Wakulla County, FL, flood risk for displaced and sheltered people is low even though the flood hazard is relatively high and on par with portions of Mississippi and Alabama. However, Wakulla County has a significantly lower population density.

The average increase in displaced people across the NGOM is 8,056 people per meter of SLR, and people requiring shelter is 300 per meter of SLR. This does not include increases in populations or new development. Under the (plausible) intermediate-high SLR scenario (1.2 m), the number of additional displaced people per decade would increase by 1,208 (or 121 per year from 2020 to 2100). This value would be as high as 3,483 people per decade in Jackson County, MS (or 348 per year).

4. Discussion and Conclusions

Considering the cost of natural disasters, the increasing population, and aging infrastructure it is of paramount importance to increase resilience, thus increasing the ability of communities to prepare, plan for, absorb, recover from, or more successfully adapt to actual or potential adverse events through preventative action (National

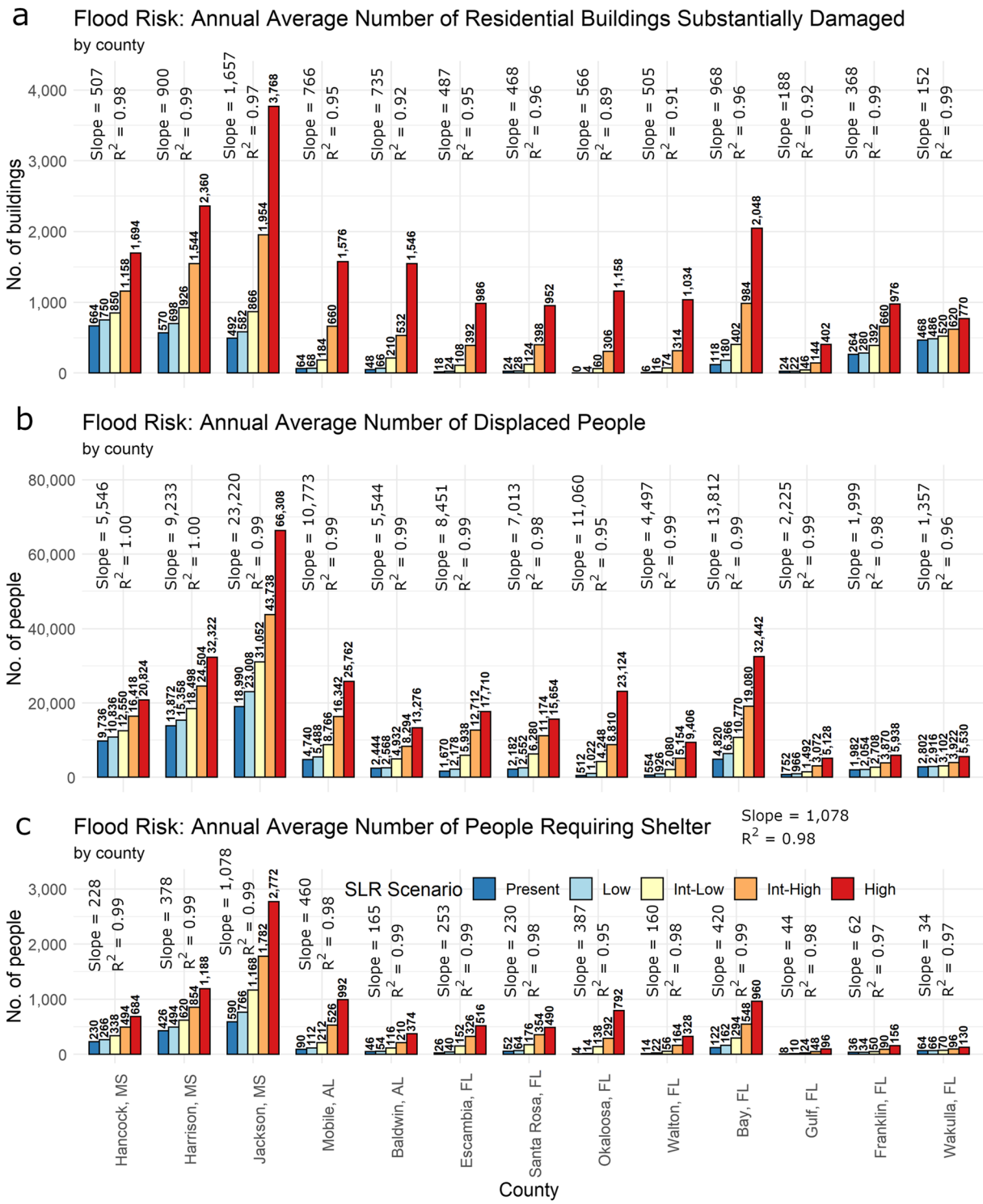

Figure 8. Flood risk as quantified by the annual average number of (a) buildings substantially damaged, (b) displaced people, and (c) people requiring shelters. The population values are categorized by county and sea level rise (SLR) scenario. The linear regression line slope and its R^2 value are shown for each county as function of the SLR amount. The slope in (a) is number of substantially damaged buildings per meter of SLR, (b) is the number of displaced people per meter of SLR, and (c) is the number of people requiring shelter per meter of SLR.

Research Council, 2012). One tenant in building resilience is to manage future change instead of steady-state or historical baselines (Chapin et al., 2009). Thus, it is essential to consider the potential for increased risk as a result of human development, changing landscapes and ecosystems, and SLR all happening at once (Batten et al., 2008; Blais et al., 2006; Brody et al., 2013; Galloway et al., 2006; Habete & Ferreira, 2017). Although other studies have assessed the potential increase in impacts to infrastructure from storm surge under SLR (Frazier et al., 2010; Shepard et al., 2012), these studies have focused on a single storm scenario or a range of scenarios following the Saffir-Simpson scale. The Saffir-Simpson scale approach is limited. It does not reflect the wide range of potential flood depths and extent outcomes for various hydrodynamics factors associated with surge generation (Irish & Resio, 2010). In addition, the Saffir-Simpson scale is a metric to classify tropical cyclone intensity based on wind speeds (1-min sustained) and not a method to quantify the probability of a region to experience flooding, which is problematic when quantifying flood probabilities and risk. Therefore, such approaches are limited in their application and stop short of flood risk quantification.

Previous work on CDSLR across the NGOM presented improved flood hazard results when incorporating future LULC and morphology driven by increased carbon emissions and SLR (Bilskie et al., 2014; Bilskie et al., 2019). The results in this work highlight the varying levels of risk across the NGOM and the change in risk under climate change-induced impacts, including SLR, landscape change (including marsh loss and upland migration, shoreline/barrier island morphology), and urbanization (land use land cover change). We found that different counties face disparities in building damage and socio-economic risk. Thus, resilience planning is not a one-size-fits-all and requires localized prioritization and actions.

First, we have shown it is possible to use our novel CDSLR framework to assess flood risk at the census block level for a multi-state coastal region using results from a contemporary, high-resolution, numerical hurricane storm surge model. Our focus on flood risk quantification is not on monetary losses but on actual impacts such as property damages, displaced people, and people requiring shelter. One of the major direct socio-economic impacts due to storm surge are losses associated with the built environment. Loss of homes has reverberating impacts in a community and can result in several social and health effects such as financial impacts, stress, and anxiety (Carroll et al., 2009; Cox et al., 2002). This study demonstrates that the increase in flood damage associated with increasing sea level scenarios makes it necessary for emergency managers to plan for the future rather than the current reality.

Second, we found that residential buildings located in census blocks already within the 1% AEP floodplain substantially increase flood risk more than those that become inundated in the future as the envelope of the 1% AEP floodplain expands. As sea level increases, these homes become 100% damaged, and (i.e., total loss) flood risk reaches a ceiling. These total-loss scenarios can impact the ability of homeowners to rebuild after such an event. For example, a study by Turnham et al. (2011) found that buildings with extensive flood damage were 39% less likely to be rebuilt in the aftermath of Hurricane Katrina. It is essential to consider that rebuilding after a total loss may be beyond the coverage of the National Flood Insurance Program (NFIP) limits ($250,000 for the building and $100,000 for the building contents [https://www.floodsmart.gov/flood-insurance/types]). Also, a 2019 report found that many communities in areas of extreme risk to natural hazards (such as the Atlantic and Gulf Coasts) can suffer from underinsurance as a result of increasing building and labor costs that may not be factored into the insurance valuation and coverage estimates (Nothaft et al., 2019). The impacts of underinsurance have recently been observed in California wildfires over the last few years, where 80% of affected homes were underinsured (Adriano, 2018). Catastrophic losses can have long-term impacts on the economic health of individuals, increasing the amount of debt and resulting in lower credit scores for years after the event (Ratcliffe et al., 2019).

Third, flood risk linearly increased for the annual average number of residential buildings across the SLR scenarios. This is counter-intuitive, especially given the non-linear increase in flood depths as SLR increases. The linear increase results from the depth-damage relationships employed within HAZUS (DHS and Federal Emergency Management Agency; Scawthorn et al., 2006). The depth-damage curve is relatively linear, which results in a linear increase in damaged buildings under different flood depths. Additionally, the number of buildings is not equally distributed across the landscape. Therefore, the most substantial outcome of SLR on storm surge flooding is the increase in flood depth. The additional floodplain does not exponentially expose more buildings as most in the study area are already within the 0.2% AEP floodplain. Although the number of buildings damaged does not increase exponentially, the damage cost does due to the buildings already exposed facing a greater percent in damages. Similarly, the number of displaced people and people requiring shelter also had a linear increase. It is

important to note that this may not be the case if more detailed and fine-grained depth-damage relationships and population data were incorporated into HAZUS. It is also important to note that aggregating the flood risk data by county is also a factor in the linear increase.

The approach applied herein can be used to develop actionable and informational material for planners and emergency managers who want to understand better the current and future flood risk, particularly in locations outside the existing floodplain where there is the option for voluntary flood insurance. Most of the Federal Flood Insurance policies are held within the Special Flood Hazard (SFHA) area (100 year floodplain). Uptake in the coastal counties presented in this study vary from 20% to 80%, yet outside the SFHA the flood insurance uptake rate can be very low. Thus, as the flood risk increases under SLR, the probability of homeowners experiencing a catastrophic loss will rise both inside and outside SFHA. In addition to insurance and reconstruction concerns, public assistance and infrastructure will be needed to temporarily house displaced people or people with homes that are severely damaged for an extended period. In addition, people who suffer from severely damaged homes are likely to need financial disaster assistance and aid in navigating the application process while also dealing with additional financial issues and health problems (Hamel et al., 2018).

Some limitations to this study should be noted. First, we do not consider the effects of local wave run up, damage due to winds, impacts of sea surface warming, and tropical cyclone climatology. New research argues that warming and changes to storm climatology in the Gulf of Mexico can have local effects on storm surge heights (Knutson et al., 2020; Marsooli et al., 2019; Zhang & Li, 2019). These implications would likely increase the number of damaged buildings; however, since we use present-day hazard results as a baseline, our major conclusions and implications would not change. Second, while our biogeophysical modeling considered future SLR scenarios and coastal dynamics, the human environment is based on current conditions. We did not directly consider new development or future populations on risks beyond considering land use land cover changes according to each SLR scenario. With the continuing upward trend of coastal development worldwide, flood risk and impacts may increase (Bouwer, 2011; Muis et al., 2016). However, coastal regions with declining growth trends should also be addressed, such as declining growth trends that are not well documented in the literature. Therefore, future studies should more directly incorporate projections of future populations and development as increased economic exposure is likely to be the greatest driver of coastal risk (Reguero et al., 2018). For example, flood risk in Jefferson County may increase and look similar to Jackson County, given a future increase in population and residential development.

Third, this work is limited by the quality of flood depth-damage relationships. Depth-damage relationships can vary widely across locations and building types. In addition, the quality of the building type classification in HAZUS is limited, which determines which cures are applied (occupancy type, number of floors, apartment, manufactured home, etc.) Therefore, the depth-damage functions can significantly impact the final damage assessment results. Recent work by Wing et al. (2020) has improved depth-damage functions using over 2 million NFIP data claims attempts to resolve some of these shortcomings. It would be ideal to use census-block depth-damage relationships if they exist, but this is a challenging task.

Fourth, a natural extension of this work should assess the flood risk uncertainty. There is uncertainty in the derivation of the synthetic storm set, hydrodynamic model, SLR scenarios, morphology, and depth-damage relationships, among others, which should be investigated in future work. However, the results and patterns discussed in this work highlight changes in flood risk under future SLR conditions.

The hazard and exposure modeling framework conducted herein is not specific to the NGOM region. Such efforts can be translated to other shorelines, both coastal and riverine.

Data Availability Statement

All data for this paper is appropriately cited and referred to in the reference list. The return period stillwater elevation data can be found at the following (Bilskie et al., 2018): https://coastalscience.noaa.gov/data_reports/nccos-ecological-effects-sea-level-rise-northern-gulf-mexico-eeslr-ngom-simulated-return-period-stillwater-elevation-ncei-accession-0170340/. GIS and *R* datafiles for the damage buildings, displaced people, and people requiring shelter can be found at the following (Bilskie et al., 2022) https://github.com/mattbilskie/2022EF_NGOM_Flood_Risk.

Acknowledgments
This research was funded under award NA10NOS4780146 and award NA16NOS4780208 from the National Oceanic and Atmospheric Administration (NOAA) Center for Sponsored Coastal Ocean Research (CSCOR) and the Louisiana Sea Grant Laborde Chair. In addition, this publication was made possible, in part, by the National Oceanic and Atmospheric Administration Office of Education Educational Partnership Program award (NA16SEC4810009). This work used the Extreme Science and Engineering Discovery Environment (XSEDE), which is supported by the National Science Foundation (NSF) Grant No. ACI-1053575. This work also used High-Performance Computing at Louisiana State University and the Louisiana Optical Network Initiative. The contents herein are solely the authors' responsibility and do not necessarily represent the official views of the U.S. Department of Commerce, National Oceanic and Atmospheric Administration Louisiana, Louisiana Sea Grant, XSEDE, National Science Foundation, Louisiana State University, or the Louisiana Optical Network Initiative. The authors thank the two reviewers for their time in reviewing the manuscript and providing feedback. The authors dedicated this work to the memory of our friend, mentor, and colleague, Dr. Scott C. Hagen.

References

Adriano, L. (2018). *Wildfire victims are largely underinsured*. Insurance Business America.

Alizad, K., Hagen, S. C., Medeiros, S. C., Bilskie, M. V., Morris, J. T., Balthis, L., & Buckel, C. A. (2018). Dynamic responses and implications to coastal wetlands and the surrounding regions under sea level rise. *PLoS One*, *13*(10), e0205176. https://doi.org/10.1371/journal.pone.0205176

Alizad, K., Hagen, S. C., Morris, J. T., Bacopoulos, P., Bilskie, M. V., Weishampel, J. F., & Medeiros, S. C. (2016). A coupled, two-dimensional hydrodynamic-marsh model with biological feedback. *Ecological Modelling*, *327*, 29–43. https://doi.org/10.1016/j.ecolmodel.2016.01.013

Alizad, K., Hagen, S. C., Morris, J. T., Medeiros, S. C., Bilskie, M. V., & Weishampel, J. F. (2016). Coastal wetland response to sea-level rise in a fluvial estuarine system. *Earth's Future*, *4*(11), 483–497. https://doi.org/10.1002/2016EF000385

Banks, J. C., Camp, J. V., & Abkowitz, M. D. (2014). Adaptation planning for floods: A review of available tools. *Natural Hazards*, *70*(2), 1327–1337. https://doi.org/10.1007/s11069-013-0876-7

Batten, B. K., Weberg, P., Mampara, M., & Xu, L. (2008). Evaluation of sea level rise for FEMA flood insurance studies: Magnitude and time-frames of relevance. In *Solutions to coastal disasters 2008*, pp. 62–72. https://doi.org/10.1061/40968(312)6

Bilskie, M., Angel, D. D., Yoskowitz, D., & Hagen, S. C. (2022), *Flood risk data set for the Northern Gulf of Mexico*.

Bilskie, M. V., Coggin, D., Hagen, S. C., & Medeiros, S. C. (2015). Terrain-driven unstructured mesh development through semi-automatic vertical feature extraction. *Advances in Water Resources*, *86*, 102–118. https://doi.org/10.1016/j.advwatres.2015.09.020

Bilskie, M. V., & Hagen, S. C. (2013). Topographic accuracy assessment of bare Earth Lidar-derived unstructured meshes. *Advances in Water Resources*, *52*, 165–177. https://doi.org/10.1016/j.advwatres.2012.09.003

Bilskie, M. V., & Hagen, S. C. (2018). Defining flood zone transitions in low-gradient coastal regions. *Geophysical Research Letters*, *45*(6), 2761–2770. https://doi.org/10.1002/2018GL077524

Bilskie, M. V., Hagen, S. C., Alizad, K., Medeiros, S. C., Passeri, D. L., Needham, H. F., & Cox, A. (2016). Dynamic simulation and numerical analysis of hurricane storm surge under sea level rise with geomorphologic changes along the Northern Gulf of Mexico. *Earth's Future*, *4*(5), 177–193. https://doi.org/10.1002/2015EF000347

Bilskie, M. V., Hagen, S. C., & Irish, J. L. (2019). Development of return period stillwater floodplains for the Northern Gulf of Mexico under the coastal dynamics of sea level rise. *Journal of Waterway, Port, Coastal, and Ocean Engineering*, *145*(2), 04018043. https://doi.org/10.1061/(ASCE)WW.1943-5460.0000468

Bilskie, M. V., Hagen, S. C., Medeiros, S., Kidwell, D., Buckel, C., & Passeri, D. (2018). NCCOS ecological effects of sea level rise in the Northern Gulf of Mexico (EESLR-NGOM): Simulated return period stillwater elevation (NCEI accession 0170340) Dataset. *NOAA National Centers for Environmental Information*.

Bilskie, M. V., Hagen, S. C., Medeiros, S. C., Cox, A. T., Salisbury, M., & Coggin, D. (2016). Data and numerical analysis of astronomic tides, wind-waves, and hurricane storm surge along the Northern Gulf of Mexico. *Journal of Geophysical Research: Oceans*, *121*(5), 3625–3658. https://doi.org/10.1002/2015JC011400

Bilskie, M. V., Hagen, S. C., Medeiros, S. C., & Passeri, D. L. (2014). Dynamics of sea level rise and coastal flooding on a changing landscape. *Geophysical Research Letters*, *41*(3), 927–934. https://doi.org/10.1002/2013GL058759

Blais, N. C., Nguyen, Y., Tate, E., Dogan, F., Samant, L., Mifflin, E., & Jones, C. (2006). *Managing future development conditions in the national flood insurance Program*.

Booij, N., Ris, R. C., & Holthuijsen, L. H. (1999). A third-generation wave model for coastal regions 1. Model description and validation. *Journal of Geophysical Research*, *104*(C4), 7649–7666. https://doi.org/10.1029/98JC02622

Bouwer, L. M. (2011). Have disaster losses increased due to Anthropogenic climate change? *Bulletin of the American Meteorological Society*, *92*(1), 39–46. https://doi.org/10.1175/2010bams3092.1

Brody, S. D., Blessing, R., Sebastian, A., & Bedient, P. (2013). Delineating the reality of flood risk and loss in Southeast Texas. *Natural Hazards Review*, *14*(2), 89–97. https://doi.org/10.1061/(ASCE)NH.1527-6996.0000091

Carroll, B., Morbey, H., Balogh, R., & Araoz, G. (2009). Flooded homes, broken bonds, the meaning of home, psychological processes and their impact on psychological health in a disaster. *Health & Place*, *15*(2), 540–547. https://doi.org/10.1016/j.healthplace.2008.08.009

Chapin, F. S., III., Kofinas, G. P., & Folke, C. (2009). A framework for understanding change. In F. S. ChapinIII, G. P. Kofinas, & C. Folke (Eds.), *Principles of ecosystem Stewardship: Resilience-based natural resource management in a changing world* (pp. 3–28). Springer-Verlag. https://doi.org/10.1007/978-0-387-73033-2_1

Cox, D., Hunt, J., Mason, P., Wheater, H., Wolf, P., Tapsell, S. M., et al. (2002). Vulnerability to flooding: Health and social dimensions. *Philosophical Transactions of the Royal Society of London, Series A: Mathematical, Physical and Engineering Sciences*, *360*(1796), 1511–1525. https://doi.org/10.1098/rsta.2002.1013

Dawson, C., Westerink, J. J., Feyen, J. C., & Pothina, D. (2006). Continuous, discontinuous and coupled discontinuous–continuous Galerkin finite element methods for the shallow water equations. *International Journal for Numerical Methods in Fluids*, *52*(1), 63–88. https://doi.org/10.1002/fld.1156

DeLorme, D. E., Kidwell, D., Hagen, S. C., & Stephens, S. H. (2016). Developing and managing transdisciplinary and transformative research on the coastal dynamics of sea level rise: Experiences and lessons learned. *Earth's Future*, *4*(5), 194–209. https://doi.org/10.1002/2015EF000346

Dietrich, J. C., Zijlema, M., Westerink, J. J., Holthuijsen, L. H., Dawson, C. N., Luettich, R. A., et al. (2011). Modeling hurricane waves and storm surge using integrally-coupled, scalable computations. *Coastal Engineering*, *58*, 45–65. https://doi.org/10.1016/j.coastaleng.2010.08.001

Federal Emergency Management Agency (FEMA) (2013). *Hazus-MH flood model user Manual*.

Frazier, T. G., Wood, N., Yarnal, B., & Bauer, D. H. (2010). Influence of potential sea level rise on societal vulnerability to hurricane storm-surge hazards, Sarasota County, Florida. *Applied Geography*, *30*(4), 490–505. https://doi.org/10.1016/j.apgeog.2010.05.005

Galloway, G. E., Baecher, G. B., Plasencia, D., Coulton, K. G., Louthain, J., Bagha, M., & Levy, A. R. (2006). *Assessing the adequacy of the national flood insurance program's 1 percent flood Standard, water policy collaborative*. University of Maryland.

Genovese, E., Hallegatte, S., & Dumas, P. (2011). Damage assessment from storm surge to coastal cities: Lessons from the Miami area. In S. Geertman, W. Reinhardt, & F. Toppen (Eds.), *Advancing geoinformation science for a changing world* (pp. 21–43). Springer Berlin Heidelberg. https://doi.org/10.1007/978-3-642-19789-5_2

Habete, D., & Ferreira, C. M. (2017). Potential impacts of sea-level rise and land-use change on special flood hazard areas and associated risks. *Natural Hazards Review*, *18*(4), 04017017. https://doi.org/10.1061/(ASCE)NH.1527-6996.0000262

Hagen, S. C., & Bacopoulos, P. (2012). Coastal flooding in Florida's big Bend region with application to sea level rise based on synthetic storms analysis. *Terrestrial, Atmospheric and Oceanic Sciences*, *23*, 481–500. (WMH). https://doi.org/10.3319/tao.2012.04.17.01(wmh)

Hagen, S. C., Passeri, D. L., Bilskie, M. V., DeLorme, D. E., & Yoskowitz, D. (2017). Systems approaches for coastal hazard assessment and resilience, In *Oxford research Encyclopedia of natural hazard Science*. https://doi.org/10.1093/acrefore/9780199389407.013.28

Hallegatte, S. (2007). The use of synthetic hurricane tracks in risk analysis and climate change damage assessment. *Journal of Applied Meteorology and Climatology*, *46*(11), 1956–1966. https://doi.org/10.1175/2007jamc1532.1

Hallegatte, S., Green, C., Nicholls, R. J., & Corfee-Morlot, J. (2013). Future flood losses in major coastal cities. *Nature Climate Change*, *3*, 802–806. https://doi.org/10.1038/nclimate1979

Hamel, L., Wu, B., Brodie, M., Sim, S., & Marks, E. (2018). *One year after the storm: Texas Gulf coast residents' views and experiences with hurricane Harvey Recovery*. Kaiser Family Foundation Report 9225.

Heberger, M., Cooley, H., Herrera, P., Gleick, P. H., & Moore, E. (2011). Potential impacts of increased coastal flooding in California due to sea-level rise. *Climatic Change*, *109*(1), 229–249. https://doi.org/10.1007/s10584-011-0308-1

Highfield, W. E., Norman, S. A., & Brody, S. D. (2013). Examining the 100 year floodplain as a metric of risk, loss, and household adjustment. *Risk Analysis*, *33*(2), 186–191. https://doi.org/10.1111/j.1539-6924.2012.01840.x

Irish, J., & Resio, D. T. (2010). A forensic analysis of hurricane Katrina's impact: Methods and findings. *Ocean Engineering*, *37*(1), 69–81. https://doi.org/10.1016/j.oceaneng.2009.07.012

Irish, J. L., Frey, A. E., Rosati, J. D., Olivera, F., Dunkin, L. M., Kaihatu, J. M., et al. (2010). Potential implications of global warming and barrier island degradation on future hurricane inundation, property damages, and population impacted. *Ocean & Coastal Management*, *53*(10), 645–657. https://doi.org/10.1016/j.ocecoaman.2010.08.001

Jongman, B., Ward, P. J., & Aerts, J. C. J. H. (2012). Global exposure to river and coastal flooding: Long term trends and changes. *Global Environmental Change*, *22*(4), 823–835. https://doi.org/10.1016/j.gloenvcha.2012.07.004

Kennedy, A. B., Gravois, U., Zachry, B. C., Westerink, J. J., Hope, M. E., Luettich, R. A., & Dean, R. G. (2011). Origin of the hurricane Ike forerunner surge. *Geophysical Research Letters*, *38*(8), L08608. https://doi.org/10.1029/2011gl047090

Kidwell, D. M., Dietrich, J. C., Hagen, S. C., & Medeiros, S. C. (2016). An Earth's future special collection: Impacts of the coastal dynamics of sea level rise on low gradient coastal landscapes. *Earth's Future*, *5*, 2–9. https://doi.org/10.1002/2016EF000493

Kinnmark, I. (1985). The shallow water wave equations: Formulation, analysis, and application. In *Lecture notes in engineering*. Springer-Verlag.

Knutson, T., Camargo, S. J., Chan, J. C. L., Emanuel, K., Ho, C.-H., Kossin, J., et al. (2020). Tropical cyclones and climate change assessment: Part II: Projected response to anthropogenic warming. *Bulletin of the American Meteorological Society*, *101*(3), E303–E322. https://doi.org/10.1175/bams-d-18-0194.1

Kolar, R. L., Gray, W. G., Westerink, J. J., Cantekin, M. E., & Blain, C. A. (1994). Aspects of nonlinear simulations using shallow-water models based on the wave continuity equation. *Computers & Fluids*, *23*(3), 523–538. https://doi.org/10.1016/0045-7930(94)90017-5

Kron, W. (2005). Flood risk = hazard • values • vulnerability. *Water International*, *30*(1), 58–68. https://doi.org/10.1080/02508060508691837

Linkov, I., Bridges, T., Creutzig, F., Decker, J., Fox-Lent, C., Kroger, W., et al. (2014). Changing the resilience paradigm. *Nature Climate Change*, *4*(6), 407–409. https://doi.org/10.1038/nclimate2227

Liu, Y., Asher, T. G., & Irish, J. L. (2019). Physical drivers of changes in probabilistic surge hazard under sea level rise. *Earth's Future*, *7*(7), 819–832. https://doi.org/10.1029/2019EF001216

Luettich, R. A., & Westerink, J. J. (2004), *Formulation and numerical implementations of the 2D/3D ADCIRC finite element model version 44*, 12–08.

Marsooli, R., Lin, N., Emanuel, K., & Feng, K. (2019). Climate change exacerbates hurricane flood hazards along US Atlantic and Gulf Coasts in spatially varying patterns. *Nature Communications*, *10*(1), 3785. https://doi.org/10.1038/s41467-019-11755-z

Medeiros, S., Hagen, S., Weishampel, J., & Angelo, J. (2015). Adjusting Lidar-derived digital terrain models in coastal marshes based on estimated aboveground biomass density. *Remote Sensing*, *7*(4), 3507–3525. https://doi.org/10.3390/rs70403507

Merz, B., Kreibich, H., Schwarze, R., & Thieken, A. (2010). Review article "Assessment of economic flood damage". *Natural Hazards and Earth System Sciences*, *10*(8), 1697–1724. https://doi.org/10.5194/nhess-10-1697-2010

Messner, F., & Meyer, V. (2006). *Flood damage, vulnerability and risk perception—Challenges for flood damage research*. Springer Netherlands.

Meyer, V., Haase, D., & Scheuer, S. (2009). Flood risk assessment in European river basins—Concept, methods, and challenges exemplified at the Mulde river. *Integrated Environmental Assessment and Management*, *5*(1), 17–26. https://doi.org/10.1897/IEAM_2008-031.1

Muis, S., Verlaan, M., Winsemius, H. C., Aerts, J. C. J. H., & Ward, P. J. (2016). A global reanalysis of storm surges and extreme sea levels. *Nature Communications*, *7*, 11969. https://doi.org/10.1038/ncomms11969

National Research Council. (2012). *Disaster resilience: A national imperative* (p. 260). The National Academies Press.

Neumann, B., Vafeidis, A. T., Zimmermann, J., & Nicholls, R. J. (2015). Future coastal population growth and exposure to sea-level rise and coastal flooding - A global assessment. *PLoS One*, *10*(3), e0118571. https://doi.org/10.1371/journal.pone.0118571

Niedoroda, A. W., Resio, D. T., Toro, G. R., Divoky, D., Das, H. S., & Reed, C. W. (2010). Analysis of the coastal Mississippi storm surge hazard. *Ocean Engineering*, *37*(1), 82–90. https://doi.org/10.1016/j.oceaneng.2009.08.019

Nothaft, F., Gromowski, A., Tierney, A., Moore, D., & Kopperud, G. (2019). *Insurance coverage adequacy report: The effects of underinsurance to the property Ecosystem*. CoreLogic.

Oddo, P. C., Lee, B. S., Garner, G. G., Srikrishnan, V., Reed, P. M., Forest, C. E., & Keller, K. (2020). Deep uncertainties in sea-level rise and storm surge projections: Implications for coastal flood risk management. *Risk Analysis*, *40*(1), 153–168. https://doi.org/10.1111/risa.12888

Olsen, A. S., Zhou, Q., Linde, J. J., & Arnbjerg-Nielsen, K. (2015). Comparing methods of calculating expected annual damage in urban Pluvial flood risk assessments. *Water*, *7*(1), 255–270. https://doi.org/10.3390/w7010255

Parris, A., Bromirski, P., Burkett, V., Cayan, D., Culver, M., Hall, J., et al. (2012). *Global sea level rise scenarios for the United States National climate assessment* (p. 37).

Passeri, D. L., Hagen, S. C., Bilskie, M. V., & Medeiros, S. C. (2015). On the significance of incorporating shoreline changes for evaluating coastal hydrodynamics under sea level rise scenarios. *Natural Hazards*, *75*(2), 1599–1617. https://doi.org/10.1007/s11069-014-1386-y

Passeri, D. L., Hagen, S. C., & Irish, J. L. (2014). Comparison of shoreline change rates along the South Atlantic bight and Northern Gulf of Mexico coasts for better evaluation of future shoreline positions under sea level rise. *Journal of Coastal Research*, *68*, 20–26. https://doi.org/10.2112/SI68-003.1

Passeri, D. L., Hagen, S. C., Medeiros, S. C., & Bilskie, M. V. (2015). Impacts of historic morphology and sea level rise on tidal hydrodynamics in a microtidal estuary (Grand Bay, Mississippi). *Continental Shelf Research*, *111*, 150–158, CSR3698. https://doi.org/10.1016/j.csr.2015.08.001

Passeri, D. L., Hagen, S. C., Medeiros, S. C., Bilskie, M. V., Alizad, K., & Wang, D. (2015). The dynamic effects of sea level rise on low-gradient coastal landscapes: A review. *Earth's Future*, *3*(6), 159–181. https://doi.org/10.1002/2015EF000298

Passeri, D. L., Hagen, S. C., Plant, N. G., Bilskie, M. V., Medeiros, S. C., & Alizad, K. (2016). Tidal hydrodynamics under future sea level rise and coastal morphology in the Northern Gulf of Mexico. *Earth's Future*, *4*(5), 159–176. https://doi.org/10.1002/2015EF000332

Plant, N. G., Robert Thieler, E., & Passeri, D. L. (2016). Coupling centennial-scale shoreline change to sea-level rise and coastal morphology in the Gulf of Mexico using a Bayesian network. *Earth's Future*, *4*(5), 143–158. https://doi.org/10.1002/2015EF000331

Ratcliffe, C., Congdon, W. J., Stanczyk, A., Martin, C., & Kotapati, B. (2019). *Insult to injury: Natural disasters and Residents' financial Health*. Urban Institute.

Reguero, B. G., Beck, M. W., Bresch, D. N., Calil, J., & Meliane, I. (2018). Comparing the cost effectiveness of nature-based and coastal adaptation: A case study from the Gulf coast of the United States. *PLoS One*, *13*(4), e0192132. https://doi.org/10.1371/journal.pone.0192132

Resio, D., Irish, J., & Cialone, M. (2009). A surge response function approach to coastal hazard assessment—Part 1: Basic concepts. *Natural Hazards*, *51*(1), 163–182. https://doi.org/10.1007/s11069-009-9379-y

Resio, D. T. (2007). *White paper on estimating hurricane inundation probabilities* (p. 125). U.S. Army Engineering Research and Development Center.

Rohmer, J., Lincke, D., Hinkel, J., Le Cozannet, G., Lambert, E., & Vafeidis, A. T. (2021). Unravelling the importance of uncertainties in global-scale coastal flood risk assessments under sea level rise. *Water*, *13*(6), 774. https://doi.org/10.3390/w13060774

Scawthorn, C., Flores, P., Blais, N., Seligson, H., Tate, E., Chang, S., et al. (2006). HAZUS-MH flood loss estimation methodology. II. Damage and loss assessment. *Natural Hazards Review*, *7*(2), 72–81. https://doi.org/10.1061/(ASCE)1527-6988(2006)7:2(72)

Shepard, C., Agostini, V., Gilmer, B., Allen, T., Stone, J., Brooks, W., & Beck, M. (2012). Assessing future risk: Quantifying the effects of sea level rise on storm surge risk for the southern shores of long island, New York. *Natural Hazards*, *60*(2), 727–745. https://doi.org/10.1007/s11069-011-0046-8

Smith, J. M., Cialone, M. A., Wamsley, T. V., & McAlpin, T. O. (2010). Potential impact of sea level rise on coastal surges in Southeast Louisiana. *Ocean Engineering*, *37*, 37–47. https://doi.org/10.1016/j.oceaneng.2009.07.008

Tebaldi, C., Strauss, B. H., & Zervas, C. E. (2012). Modelling sea level rise impacts on storm surges along US coasts. *Environmental Research Letters*, *7*(1), 014032. https://doi.org/10.1088/1748-9326/7/1/014032

Toro, G. R., Resio, D. T., Divoky, D., Niedoroda, A. W., & Reed, C. (2010). Efficient joint-probability methods for hurricane surge frequency analysis. *Ocean Engineering*, *37*(1), 125–134. https://doi.org/10.1016/j.oceaneng.2009.09.004

Turnham, J., Burnett, K., Martin, C., McCall, T., Juras, R., & Spader, J. (2011). *Housing Recovery on the Gulf coast, phase II: Results of property owner survey in Louisiana, Mississippi, and Texas*. Department of Housing and Urban Development, Office of Policy Development and Research.

Westerink, J. J., Luettich, R. A., Feyen, J. C., Atkinson, J. H., Dawson, C., Roberts, H. J., et al. (2008). A basin- to channel-scale unstructured grid hurricane storm surge model applied to Southern Louisiana. *Monthly Weather Review*, *136*, 833–864. https://doi.org/10.1175/2007MWR1946.1

Wing, O. E. J., Pinter, N., Bates, P. D., & Kousky, C. (2020). New insights into US flood vulnerability revealed from flood insurance big data. *Nature Communications*, *11*(1), 1444. https://doi.org/10.1038/s41467-020-15264-2

Woodruff, J. D., Irish, J. L., & Camargo, S. J. (2013). Coastal flooding by tropical cyclones and sea-level rise. *Nature*, *504*(7478), 44–52. https://doi.org/10.1038/nature12855

Zhang, F., & Li, M. (2019). Impacts of ocean warming, sea level rise, and coastline management on storm surge in a semi enclosed bay. *Journal of Geophysical Research: Oceans*, *124*(9), 6498–6514. https://doi.org/10.1029/2019JC015445

Zijlema, M. (2010). Computation of wind-wave spectra in coastal waters with SWAN on unstructured grids. *Coastal Engineering*, *57*(3), 267–277. https://doi.org/10.1016/j.coastaleng.2009.10.011

Zuzak, C., Pluss, M., Wright, S., Kendro, H., Duff, L., & Burmester, J. (2018). *Using Hazus for mitigation planning. Federal Emergency Management Agency (FEMA)*. Retrieved from https://www.fema.gov/sites/default/files/documents/fema_using-hazus-mitigation-planning.pdf